Designation: E1931 – 16 (Reapproved 2022)

Standard Guide for Non-computed X-Ray Compton Scatter Tomography[1]

This standard is issued under the fixed designation E1931; the number immediately following the designation indicates the year of original adoption or, in the case of revision, the year of last revision. A number in parentheses indicates the year of last reapproval. A superscript epsilon (ε) indicates an editorial change since the last revision or reapproval.

1. Scope

1.1 *Purpose*—This guide covers a tutorial introduction to familiarize the reader with the operational capabilities and limitations inherent in a single non-computed X-ray Compton Scatter Tomography (CST). Also included is a brief description of the physics and typical hardware configuration for CST. This single technique is still used for a small number of inspections. This is not meant as comprehensive guide covering the variety of Compton scattering techniques that are now used for non-destructive testing and security screen screening.

1.2 *Advantages*—X-ray Compton Scatter Tomography (CST) is a radiologic nondestructive examination method with several advantages that include:

1.2.1 The ability to perform X-ray examination without access to the opposite side of the examination object;

1.2.2 The X-ray beam need not completely penetrate the examination object allowing thick objects to be partially examined. Thick examination objects become part of the radiation shielding thereby reducing the radiation hazard;

1.2.3 The ability to examine and image object subsurface features with minimal influence from surface features;

1.2.4 The ability to obtain high-contrast images from low subject contrast materials that normally produce low-contrast images when using traditional transmitted beam X-ray imaging methods; and

1.2.5 The ability to obtain depth information of object features thereby providing a three-dimensional examination. The ability to obtain depth information presupposes the use of a highly collimated detector system having a narrow angle of acceptance.

1.3 *Applications*—This guide does not specify which examination objects are suitable, or unsuitable, for CST. As with most nondestructive examination techniques, CST is highly application specific thereby requiring the suitability of the method to be first demonstrated in the application laboratory. This guide does not provide guidance in the standardized practice or application of CST techniques. No guidance is provided concerning the acceptance or rejection of examination objects examined with CST.

1.4 *Limitations*—As with all nondestructive examination methods, CST has limitations and is complementary to other NDE methods. Chief among the limitations is the difficulty in performing CST on thick sections of high-*Z* materials. CST is best applied to thinner sections of lower *Z* materials. The following provides a general idea of the range of CST applicability when using a 160 keV constant potential X-ray source:

Material	Practical Thickness Range
Steel	Up to about 3 mm (⅛ in.)
Aluminum	Up to about 25 mm (1 in.)
Aerospace composites	Up to about 50 mm (2 in.)
Polyurethane Foam	Up to about 300 mm (12 in.)

The limitations of the technique must also consider the required *X*, *Y*, and *Z* axis resolutions, the speed of image formation, image quality and the difference in the X-ray scattering characteristics of the parent material and the internal features that are to be imaged.

1.5 The values stated in both inch-pound and SI units are to be regarded separately as the standard. The values given in parentheses are for information only.

1.6 *This standard does not purport to address all of the safety concerns, if any, associated with its use. It is the responsibility of the user of this standard to establish appropriate safety, health, and environmental practices and determine the applicability of regulatory limitations prior to use.*

1.7 *This international standard was developed in accordance with internationally recognized principles on standardization established in the Decision on Principles for the Development of International Standards, Guides and Recommendations issued by the World Trade Organization Technical Barriers to Trade (TBT) Committee.*

2. Referenced Documents

2.1 *ASTM Standards:*[2]

[1] This guide is under the jurisdiction of ASTM Committee E07 on Nondestructive Testing and is the direct responsibility of E07.01 on Radiology (X and Gamma) Method.

Current edition approved June 1, 2022. Published July 2022. Originally approved in 1997. Last previous edition approved in 2016 as E1931 – 16. DOI: 10.1520/E1931-16R22.

[2] For referenced ASTM standards, visit the ASTM website, www.astm.org, or contact ASTM Customer Service at service@astm.org. For *Annual Book of ASTM Standards* volume information, refer to the standard's Document Summary page on the ASTM website.

E747 Practice for Design, Manufacture and Material Grouping Classification of Wire Image Quality Indicators (IQI) Used for Radiology
E1025 Practice for Design, Manufacture, and Material Grouping Classification of Hole-Type Image Quality Indicators (IQI) Used for Radiography
E1255 Practice for Radioscopy
E1316 Terminology for Nondestructive Examinations
E1441 Guide for Computed Tomography (CT)
E1453 Guide for Storage of Magnetic Tape Media that Contains Analog or Digital Radioscopic Data
E1475 Guide for Data Fields for Computerized Transfer of Digital Radiological Examination Data
E1647 Practice for Determining Contrast Sensitivity in Radiology

2.2 *ANSI/ASNT Standards:*[3]

SNT-TC-1A ASNT Recommended Practice for Personnel Qualification and Certification in Nondestructive Testing
ANSI/ASNT CP-189 Standard for Qualification and Certification in Nondestructive Testing Personnel

2.3 *Military Standard:*[4]

MIL-STD-410 Nondestructive Testing Personnel Qualification and Certification

2.4 *Aerospace Standard:*[5]

AIA-NAS-410 Aerospace Industries Association, National Aerospace Standard-4105 Certification and Qualification of Nondestructive Test Personnel[6]

2.5 *ISO Standard:*[7]

ISO 9712 Nondestructive Testing—Qualification and Certification of NDT Personnel

3. Terminology

3.1 *Definitions:*

3.1.1 CST, being a radiologic examination method, uses much the same vocabulary as other X-ray examination methods. A number of terms used in this standard are defined in Terminology E1316. It may also be helpful to read Guide E1441.

4. Summary of Guide

4.1 *Description*—Compton Scatter Tomography is a uniquely different nondestructive test method utilizing penetrating X-ray or gamma-ray radiation. Unlike computed tomography (CT), CST produces radioscopic images which are not computed images. Multiple slice images can be simultaneously produced so that the time per slice image is in the range of a few seconds. CST can produce images that are thin with respect to the examination object thickness (slice images) and which are at right angles to the X-ray beam. Each two-dimensional slice image (*X–Y* axes) is produced at an incremental distance along and orthogonal to the X-ray beam (*Z*–axis). A stack of CST images therefore represents a solid volume within the examination object. Each slice image contains examination object information which lies predominantly within the desired slice. To make an analogy as to how CST works, consider a book. The examination object may be larger or smaller (in length, width and depth) then the analogous book. The CST slice images are the pages in the book. Paging through the slice images provides information about examination object features lying at different depths within the examination object.

4.2 *Image Formation*—CST produces one or more digital slice plane images per scan. Multiple slice images can be produced in times ranging from a few seconds to a few minutes depending upon the examined area, desired spatial resolution and signal-to-noise ratio. The image is digital and is typically assembled by computer. CST images are free from reconstruction artifacts as the CST image is produced directly and is not a calculated image. Because CST images are digital, they may be enhanced, analyzed, archived and in general handled as any other digital information.

4.3 *Calibration Standards*—As with all nondestructive examinations, known standards are required for the calibration and performance monitoring of the CST method. Practice E1255 calibration block standards that are representative of the actual examination object are the best means for CST performance monitoring. Conventional radiologic performance measuring devices, such as Test Method E747 and Practice E1025 image quality indicators or Practice E1647 contrast sensitivity gages are designed for transmitted X-ray beam imaging and are of little use for CST. With appropriate calibration, CST can be utilized to make three-dimensional measurements of internal examination object features.

5. Significance and Use

5.1 *Principal Advantage of Compton Scatter Tomography*—The principal advantage of CST is the ability to perform three-dimensional X-ray examination without the requirement for access to the back side of the examination object. CST offers the possibility to perform X-ray examination that is not possible by any other method. The CST sub-surface slice image is minimally affected by examination object features outside the plane of examination. The result is a radioscopic image that contains information primarily from the slice plane. Scattered radiation limits image quality in normal radiographic and radioscopic imaging. Scatter radiation does not have the same detrimental effect upon CST because scatter radiation is used to form the image. In fact, the more radiation the examination object scatters, the better the CST result. Low subject contrast materials that cannot be imaged well by conventional radiographic and radioscopic means are often excellent candidates for CST. Very high contrast sensitivities and excellent spatial resolution are possible with CST tomography.

[3] Available from American National Standards Institute (ANSI), 25 W. 43rd St., 4th Floor, New York, NY 10036, http://www.ansi.org.
[4] Available from Standardization Documents Order Desk, DODSSP, Bldg. 4, Section D, 700 Robbins Ave., Philadelphia, PA 19111-5098, http://www.dodssp.daps.mil.
[5] Available from Federal Aviation Administration (FAA), 800 Independence Ave., SW, Washington, DC 20591, http://www.faa.gov.
[6] This document has superseded MIL-STD-410; however, MIL-STD-410 is still acceptable to the FAA
[7] Available from International Organization for Standardization (ISO), ISO Central Secretariat, BIBC II, Chemin de Blandonnet 8, CP 401, 1214 Vernier, Geneva, Switzerland, http://www.iso.org.

5.2 *Limitations*—As with any nondestructive testing method, CST has its limitations. The technique is useful on reasonably thick sections of low-density materials. While a 25 mm (1 in.) depth in aluminum or 50 mm (2 in.) in plastic is achievable, the examination depth is decreased dramatically as the material density increases. Proper image interpretation requires the use of standards and examination objects with known internal conditions or representative quality indicators (RQIs). The examination volume is typically small, on the order of a few cubic inches and may require a few minutes to image. Therefore, completely examining large structures with CST requires intensive re-positioning of the examination volume that can be time-consuming. As with other penetrating radiation methods, the radiation hazard must be properly addressed.

6. Basis of Application

6.1 Personnel Qualification is subject to contractual agreement between the parties using or referencing this standard.

6.1.1 If specified in the contractual agreement, personnel performing examinations to this standard shall be qualified in accordance with a nationally or internationally recognized NDT personnel qualification practice or standard such as ANSI/ASNT-CP-189, SNT-TC-1A, NAS-410, MIL-STD-410E, ISO 9712, or a similar document and certified by the employer or certifying agency, as applicable. The practice or standard used and its applicable revision shall be identified in the contractual agreement between the using parties.

7. Technical Description

7.1 *General Description of Compton Scatter Tomography*—Transmitted beam radiologic techniques used in radiography, radioscopy and computed tomography have dominated the use of penetrating radiation for industrial nondestructive examination. The transmitted beam technique depends upon the penetrating radiation attenuation mechanisms of photoelectric absorption and Compton scattering. For low- Z materials at energies up to about 50 keV, the photoelectric effect is the dominant attenuation mechanism. As X-ray energy increases, Compton scattering becomes the dominant attenuation mechanism. Pair production comes into play above 1.02 MeV and can become the dominant effect for higher X-ray energies. The following relationships are plotted in Fig. 1 and show the approximate dependence of the photoelectric effect and Compton scattering upon target material atomic number (Z) and incident X-ray energy (E):

The terms τ, σ, and κ represent the cross sections of the photoelectric, Compton scatter and pair-production interaction of a given X-ray photon that has energy level E. There is no analytic expression for the probability of photoelectric absorption as it varies as a function of E and Z. For the gamma and X-ray energies of interest, the exponent of Z can vary between 4 and 5.[8] The green lines are contours where the indicated cross sections are equal. Since the cross sections are proportional to the probability of the particular type of interaction,

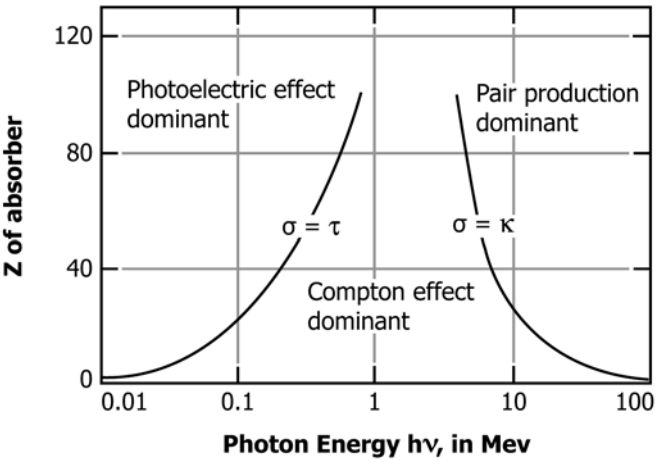

FIG. 1 Relationship Between Photoelectric, Compton, and Pair Production Effects

Photoelectric Effect: $\tau = Z^{5} / E^{7/2}$
Compton Scattering: $\sigma = Z / E$
Pair Production : $\kappa = Z^{2}$ (ln E - constant)

moving left to right in the graph, the green lines represent the boundaries of the regions where the photoelectric, Compton and pair-production events are dominant, respectively. The graph is useful for understanding the X-ray properties of a material, by knowing its predominant mass number Z. For example, it could be used to estimate its interaction regime based on the Z of the material and energy of interrogation photons.

7.1.1 CST is best suited for lower Z materials such as aluminum (Z=13) using a commercially available 160 keV X-ray generating system. Somewhat higher Z materials may be examined by utilizing a higher energy X-ray generator rated at 225, 320, or 450 keV.

7.1.2 It is useful to envision the CST process as one where the X-rays that produce the CST image originate from many discrete points within the examined volume. Each Compton scatter event generates a lower energy X ray that emanates from the scattering site. Singly scattered X rays that reach the detector carry information about the examination object material characteristics at the site where it was generated. The scatter radiation is also affected by the material through which it passes on the way to the detector. The external source of primary penetrating radiation, that may be either X rays or gamma rays, interact by the Compton scattering process. The primary radiation must have adequate energy and intensity to generate sufficient scattered radiation at the examination site to allow detection. The examination depth is limited to that depth from which sufficient scattered radiation can reach the detector to form a usable image. The examination object is therefore effectively imaged from the inside out. The CST image is formed voxel (volume element) by voxel in raster fashion where the detector's field-of-view intersects with the central X-ray beam at the examination site. The primary radiation beam source and scattered radiation detector are highly collimated to assure collection of single-scattered radiation from a known small volume of the examination object. Multiple scattered radiation causes a loss of spatial resolution, but can

[8] Knoll, G. F., *Radiation Detection and Measurement*, 3rd Ed. John Wiley and Sons, New York, 2000.

enhance contrast of features. Moving the intersection of the radiation source and detector lines of sight in a systematic fashion allows a tomogram, or slice image to be produced. Changing the distance at which the radiation source and detector lines of sight intersect allows the tomogram to be produced at a selected depth below the examination object surface.

7.2 *Significant Differences in the Transmitted Beam and Compton Scattered X-Ray Imaging Techniques*—The differences between conventional transmitted beam and Compton Scatter Imaging are so significant that CST must be considered a separate examination technique. For transmitted beam techniques, the radiation source characteristics must be carefully controlled. The energy and intensity must be selected carefully to fully penetrate the object and provide the required contrast sensitivity. Thick sections of high-density materials require a high-energy radiation source while thin sections of low-density materials require a low-energy radiation source. For CST applications, the energy and intensity of the primary radiation beam is relatively less important. The primary radiation beam energy and intensity are not critical as long as they remain stable and are sufficient to generate adequate scatter radiation at the CST examination depth. Small focal spot size is critical to transmitted beam image sharpness. The primary radiation focal spot size is also of significant importance for CST. For CST the beam must be collimated. A smaller focal spot can have a shorter collimator to achieve the same level of collimation. The $1/R^2$ (where R is the distance from the object) effect for X-ray source allows a high power, small focal spot X-ray tube (1.0 mm X-ray focal spot size (FOC) at 1800 W), to have a higher flux than a standard X-ray tube (5.5 mm FOC at 3000W) while maintaining the same image quality. For this reason an X-ray source is often a better choice than a radioisotope for CST. Radiation detection and other image forming considerations may also differ substantially from other radiologic imaging methods.

7.3 *Theory of Compton Scatter Tomography*—In the energy range appropriate for CST (roughly 50 keV to 1 MeV), the primary interaction mechanisms between electromagnetic radiation and matter are photoelectric absorption and inelastic (Compton) scatter. Fig. 2 illustrates the principles of photoelectric absorption and Compton scattering. As an X ray having an energy E_0 collides with an electron, the electron absorbs energy from the incoming X-ray photon and is ejected from its shell. In the case of photoelectric absorption, the incoming photon's energy is totally absorbed. As the energy E_0 of the incoming photon increases, the probability of photoelectric absorption decreases while the probability of Compton scattering increases. The Compton scattering creates a new X ray having and energy E', and travelling at an angle θ with respect to the direction of the original primary X ray.

7.3.1 Material linear attenuation coefficients due to photoelectric absorption and Compton scattering vary with energy. The linear absorption coefficient μ_τ falls sharply with increasing energy, while the scatter coefficient μ_σ remains nearly constant. For low-*Z* materials, scatter begins to dominate photoelectric absorption at primary radiation energies above 50 keV allowing the use of scatter radiation instead of the attenuated primary beam radiation for imaging purposes. It should also be noted that unlike the linear attenuation

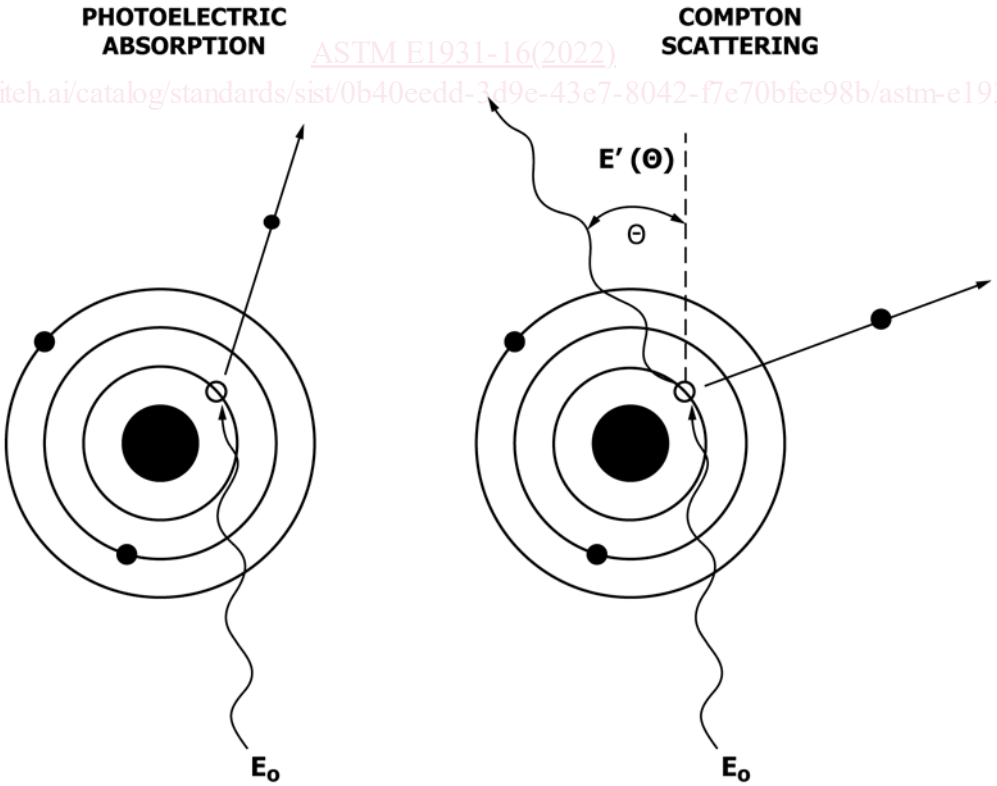

FIG. 2 Principles of Photoelectric Absorption and Compton Scattering

coefficient, the scatter coefficient is relatively independent of the primary penetrating radiation energy E_0. Many of the restrictions on energy selection associated with transmitted beam techniques are not a consideration with CST. For example, low-density aerospace composite materials can be imaged at higher energies of 100 keV or more producing high contrast using CST techniques.

7.3.2 The energy of the scattered X ray is given by:

$$E' = \frac{E_0}{1+\left(\frac{E_0}{m_e c^2}\right)(1 - \cos\theta)} \quad (1)$$

where:

E' = energy of the scattered X ray,
E_0 = energy of the primary radiation photon,
c = speed of light,
$m_e c^2$ = rest energy of the electron,
m_e = electron mass, and
θ = scattering angle.

It can be seen from Eq 1 that the energy of the scatter radiation E' decreases with increasing scattering angle θ. The amount of Compton scattering in any material is proportional to its electron density.

7.3.3 Disregarding the effects of pair production that come into play above 1.02 MeV, the total attenuation is the sum of attenuation due to photoelectric absorption and Compton scattering:

$$\mu = \mu_\tau + \mu_\sigma \quad (2)$$

where μ, μ_τ, and μ_σ are the total, photoelectric-absorption and Compton scattering linear attenuation coefficients, respectively.

Fig. 3 is a polar plot of the Klein Nishina Compton scatter (free electron scattering) angular intensity at 30 and 300 keV. Although the scatter radiation angular distribution becomes more intense in the forward direction as energy increases, there is sufficient intensity at all angles to permit the technique. The detector and the primary radiation source can therefore be positioned on the same side of the examination object in this energy range.

7.3.4 The intensity of radiation I_{SC} scattered from a volume element (voxel) V_{Voxel} inside the examination object can be approximated as follows:

$$I_{SC} = \mathrm{K}\cdot n_e \cdot V_{Voxel} \cdot I_0 e^{-\mu\tau}\left(1 - e^{-\mu_c W}\right)\left(e^{-\mu' t'}\right) + M \quad (3)$$

where:

K = constant of proportionality representing the differential scatter cross-section, detector efficiencies and all other object-dependent effects,
n_e = number of electrons per unit volume acting as scatter centers,
I_0 = incident flux,
$e^{-\mu t}$ = the attenuation along the primary beam path,
$1-e^{-\mu\sigma W}$ = the fraction of photons scattered from the primary beam in a voxel of length W. The scattering voxel is the intersection of the incident pencil beam with the solid angle subtended by the detector,
dV = the volume of the scattering voxel,
W = length of the scattering voxel along the path of the pencil beam,
$\mu\sigma$ = the Compton linear attenuation coefficient, as defined earlier,
$e^{-\mu' t'}$ = the attenuation along the scattered beam path t'. μ' is the total linear attenuation coefficient of the lower energy scattered beam,
μ' = the total linear attenuation coefficient of the lower energy scattered beam, and
M = multiple scatter component originating from quanta scattered more than once outside the voxel.

The two exponential terms describe the radiation attenuation along the primary radiation beam path t as well as the scattered beam path t'. Due to the lower X-ray energy along the scatter path, μ' is not equal to μ. The last term represents the

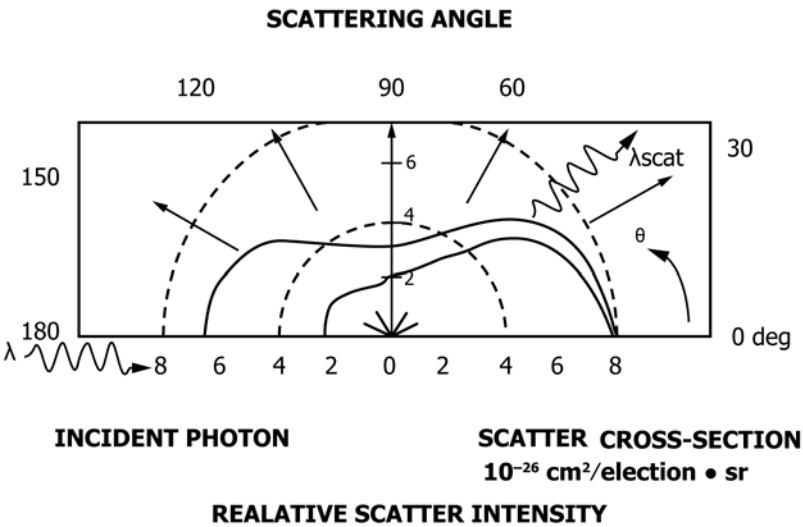

FIG. 3 Polar Plot of Relative Scatter Intensity as a Function of Scattering Angle at Primary Radiation Energies of 30 and 300 keV

contribution of photons that are scattered from other voxels, scattered more than once, and scattered into the solid angle of the pixel. The influence of this type of multiple scatter radiation needs to be minimized because it degrades the fidelity of image information corresponding to the voxel of interest, where the primary scatter originated. This may be accomplished by tightly collimating the detector to limit its field-of-view to the desired examination voxel and by software.

7.4 *Contrast Sensitivity*—One significant benefit of CST as compared with conventional transmission imaging is increased contrast sensitivity. Fig. 4 is a generalized representation of transmission beam imaging to determine the relationship between discontinuity size and subject contrast.

7.4.1 To find an expression for the sensitivity of the transmitted beam technique, consider a homogeneous material of thickness L whose attenuation coefficient is μ except for a small discontinuity region of length W and whose attenuation coefficient is μ_D.

7.4.1.1 The intensities of the radiation beams passing through the homogeneous examination object with and without the small discontinuity are I_T and $I_{T'}$, respectively, given by:

$$I_T = I_0 e^{-\mu L} \tag{4}$$

$$I_{T'} = I_0 e^{-(\mu(L - W)+\mu_D W)} \tag{5}$$

From these equations the subject contrast C is expressed as follows:

$$C = \frac{(I_{T'} - I_T)}{I_T} \times 100\,\% \tag{6}$$

$$C = \frac{e^{(-\mu(L - W)L+\mu_D W)} - e^{-\mu L}}{e^{-\mu L}} \tag{7}$$

Assuming a small discontinuity allows the exponent to be replaced by its power expansion to the first order providing the following expression:

$$C = e^{-(\mu_D - \mu)W} - 1 \tag{8}$$

$$C = (1 - (\mu_D - \mu)W) - 1 = (\mu - \mu_D)W \tag{9}$$

Thus, in a transmission imaging system, contrast is directly proportional to the discontinuity size.

7.4.2 Fig. 5 is a generalized representation of a CST system. The examination object of thickness L contains a small discontinuity of length W and having a linear attenuation coefficient of μ_D.

7.4.2.1 The CST system contrast may be determined by comparing the scatter signals, I_{SC} and $I_{SC'}$, from two similarly located voxels. For one sided radiographic inspection using backscatter imaging, the scatter signal is:[9]

$$I_{SC} = I_0 e^{-\mu_1 x_1} \mu_{scat} W e^{-\mu_2 x_2} \tag{10}$$

with μ_1 and μ_2 being the total attenuation coefficients for the entering and the scattered beam, x_1 and x_2 being the path lengths of entering and scattered beam in the base material, $\mu_{scat}W$ the probability of scatter in the scatter voxel by a material with linear scatter coefficient μ_{scat} and a thickness W. If the material in the scatter voxel at the same location changes to $\mu_{D,scat}$ the scatter signal becomes:

$$I_{sc}' = I_0 e^{-\mu_1 x_1} \mu_{D,scat} W e^{-\mu_2 x_2} \tag{11}$$

The total attenuation coefficient for the scattered beam does not change because the energy shift depends only on the scatter angle but not on the photon energy (see Eq 1). Accordingly, the contrast is:

$$C = \frac{I_{sc} - I_{sc'}}{I_{sc}} = \frac{I_0 e^{-\mu_1 x_1} \mu_{scat} W e^{-\mu_2 x_2} - I_0 e^{-\mu_1 x_1} \mu_{D,scat} W e^{-\mu_2 x_2}}{I_0 e^{-\mu_1 x_1} \mu_{scat} W e^{-\mu_{12} x_2}}$$

$$= \frac{\mu_{scat} - \mu_{D,scat}}{\mu_{scat}} \tag{12}$$

[9] Bossi, R. H., Friddell, K. D., Nelson, J. M. "Backscatter X-Ray Imaging," *Mat. Eval., 46*, 1988, pp. 1462–67.

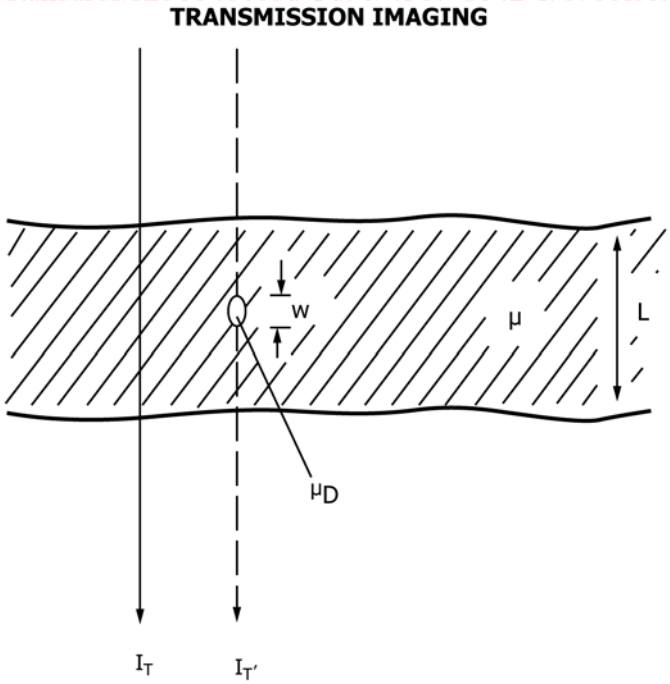

FIG. 4 Schematic Representation of the Transmitted Beam Imaging System Technique

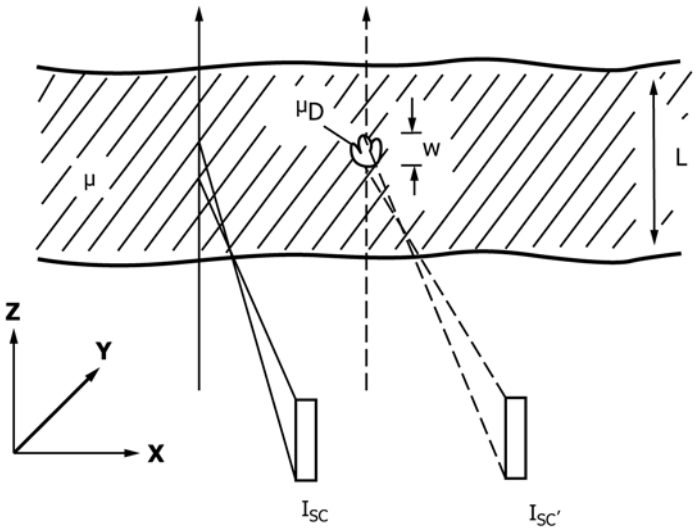

FIG. 5 Schematic Representation of the Compton Scatter Tomography Technique

Again, here μ_{scat} and $\mu_{D,scat}$ are the linear scatter coefficients in the scatter voxel.

7.4.3 CST contrast depends upon the ratio of the scattering coefficients of the parent material (μ) and the discontinuity (μ_D) and is independent of the object thickness. Assuming an air-filled discontinuity (no scatter) in aluminum with an examination voxel lying wholly within the discontinuity, scatter imaging contrast approaches 100 % for a small void. However, even a high-contrast CST image can be lost to noise if the technique is improperly applied.

7.4.4 An important consideration for CST is that the material between the scattering voxels in the region of interest and the detector must not unduly attenuate the scattered radiation or the CST signal can become so weak it is lost in the noise. Therefore, the most successful implementations of CST are those involving relatively thin sections of low-density materials where the region of interest lies relatively close to the surface.

7.5 *Sensitivity Compared to Transmission Imaging*—Transmission imaging contrast sensitivity depends upon the often very small difference between the radiation intensities of the parent material path and the parent material with discontinuity path. On the other hand, scatter imaging contrast depends upon the often large difference between the scattering coefficients of the parent material and the discontinuity. If the discontinuity is a void, it may scatter little, if any, radiation while the parent material scatters considerably thus yielding useful contrast.

7.5.1 The contrast sensitivity offered by CST can be much higher than for transmission imaging as long as the difference in the parent material and discontinuity signal is greater than the statistical fluctuations due to system and radiation noise. The higher contrast of the CST method is of practical value only if the noise levels are the same in both methods. Therefore, the contrast/noise ratio is of value for a comparison of CST and transmission imaging systems. Noise factors for transmission and CST systems, respectively, may be represented as follows:

$$\sqrt{\frac{1}{N_{trans}}} \tag{13}$$

and:

$$\sqrt{\frac{1}{N_{scat}}} \tag{14}$$

where N_{trans} and N_{scat} represent the nominal number of photons detected by the pixel element and is proportional to the exposure level, which in turn is affected by the exposure time, flux or X-ray tube filament current. These two expressions follow from considering the noise factor to be the noise to signal level, and assuming Poisson statistics. The signal power (signal level squared) divided by the noise power (i.e., the variance of the noise) is proportional to the number of photons, so the noise-to-signal level is the square root of the reciprocal of this quantity.

7.5.2 Defining the sensitivity of both CST and transmission imaging as the difference in signals in an examination object having a thickness equal to L with and without a small discontinuity at a depth L divided by the noise factor it follows:

$$S_{trans} = (\mu - \mu_D) W \sqrt{N_{trans}} \tag{15}$$

$$S_{scat} = \frac{\mu_{scat} - \mu_{D,scat}}{\mu_{scat}} \sqrt{N_{scat}} = 1 - \frac{\mu_{D,scat}}{\mu_{scat}} \sqrt{N_{scat}} \tag{16}$$

where S_{trans} and S_{scat} are the sensitivity of the transmission and CST systems, respectively.

7.6 *In-Plane Spatial Resolution*—Spatial resolution for CST can compare favorably with the radioscopic transmission imaging technique. However, it must be remembered that spatial resolution for the CST technique is a three-dimensional